

# TEMPORAL VARIABILITY FROM THE TWO-COMPONENT ADVECTIVE FLOW SOLUTION AND ITS OBSERVATIONAL EVIDENCE

BROJA G. DUTTA<sup>1,3</sup> AND SANDIP K. CHAKRABARTI<sup>2,3</sup>

*Draft version September 27, 2016*

## ABSTRACT

In the propagating oscillatory shock model, the oscillation of the post-shock region, i.e., the Compton cloud, causes the observed low-frequency quasi-periodic oscillations (QPOs). The evolution of QPO frequency is explained by the systematic variation of the Compton cloud size, i.e., the steady radial movement of the shock front, which is triggered by the cooling of the post-shock region. Thus, analysis of energy-dependent temporal properties in different variability time scales can diagnose the dynamics and geometry of accretion flows around black holes. We study these properties for the high inclination black hole source XTE J1550-564 during its 1998 outburst and the low-inclination black hole source GX 339-4 during its 2006-07 outburst using RXTE/PCA data, and we find that they can satisfactorily explain the time lags associated with the QPOs from these systems. We find a smooth decrease of the time lag as a function of time in the rising phase of both sources. In the declining phase the time lag increases with time. We find a systematic evolution of QPO frequency and hard lags in these outbursts. In XTE J1550-564, the lag changes from hard to soft (i.e., from a positive to a negative value) at a crossing frequency ( $\nu_C$ ) of  $\sim 3.4$  Hz. We present possible mechanisms to explain the lag behavior of high and low-inclination sources within the framework of a single two-component advective flow model (TCAF).

*Subject headings:* accretion, accretion disc - shock waves - stars: individual (XTE J1550-564, GX 339-4).

## 1. INTRODUCTION

The soft X-ray transient (SXT) XTE J1550-564 is one of the most interesting Galactic black hole candidates that has been studied over a broad range of wavelengths. The typical outburst behavior of XTE J1550-564 during 1998 began and ended in a low/hard state similar to the outburst profile of other black holes (e.g., GRO J1655-40, GX 339-4, etc.). This typical outburst behavior is supposedly to be due to the sudden change in viscosity in the system (Hoshi 1979, Mandal & Chakrabarti, 2010). In Chakrabarti et al. (2009, hereafter, Paper I), a systematic study of the evolution of quasi-periodic oscillation (QPO) frequencies was carried out during XTE J1550's 1998 outburst, and it was shown that the variation of the QPO frequencies during the rising and the declining phases could be understood by assuming that the centrifugal pressure supported shocks formed in the sub-Keplerian component moving in and out during the rising and declining phases, respectively, and all the while oscillating at periods comparable to the infall time scale in the post-shock region (commonly known as CENBOL or CENTrifugal barrier dominated BOundary Layer). These oscillations are primarily due to resonances occurring between the cooling time scale and the infall time scale in the CENBOL. Very recently, Chakrabarti et al. (2015) demonstrated that once the resonance sets in, it is likely to remain locked in resonance. Thus, the so-called 'Propagatory Oscillatory Shock (POS)' model of the QPO evo-

lution may indeed be valid for all such outbursting candidates.

Just as the QPO frequency variation gives us a clue to the geometry variation of the Comptonizing electron cloud, the time or phase-lag variation should also have independent information not only about the variation of geometry, but also about the energy dependent physical processes which are responsible for the emission of photons from various regions of the disc. In the present paper, we extend our study of XTE J1550-564 as presented in Papers I and II, to understand the cause of peculiarities, if any, of the time-lag behavior and its energy dependence.

In X-ray binaries (XRBs), rapid variability in the X-ray emission on time-scales of milliseconds to seconds is a common and very complex phenomenon. It was proposed (Lightman & Eardley 1974; Shakura & Sunyaev, 1976) long ago that instabilities in the standard accretion disk may cause the observed fast variability in X-ray binaries. In order to match the observation, the time variation could exist over a wide range of time-scales that depend on the range of unstable radii (Lyubarskii, 1997). Low-frequency quasi-periodic oscillations (LFQPOs) with frequencies ranging from a few mHz to  $\sim 30$  Hz are observed in black hole X-ray binaries (BHBs) (see, van der Klis 2004; Remillard & McClintock 2006). Another timing property is the manifestation of a time-lag which means a delay between the Fourier components of the hard and soft light curves (i.e., time difference in arrival times between hard and soft photons). Although time lags are observed in a large number of astronomical sources, we did not find any satisfactory explanation in the literature as to the physics of the origin(s) of this phenomenon.

<sup>1</sup> Department of Physics, Rishi Bankim Chandra College, Naihati, West Bengal, 743165, India

<sup>2</sup> S. N. Bose National Centre For Basic Sciences, Block JD, Sector - III, Salt Lake, Kolkata - 700098, India.

<sup>3</sup> Indian Centre For Space Physics, 43 Chalanika, Garia Station Road, Kolkata - 700084, India.

An early explanation of the time lag assumed that it was due to the Comptonization of soft seed photons by hot electrons, known as Compton reverberation (Payne 1980; Miyamoto et al. 1988), which naturally produces hard time lags. Several models have been proposed (e.g., Cui 1999; Poutanen 2001; Nowak et al. 1999) to explain the hard and soft lags observed in Galactic binary sources. The soft phase lags can be explained by a model (Bottcher & Liang 1999; Lin et al. 2000) in which the perturbation is assumed to propagate from the inner disk to the outer disk the soft phase lags can be explained. When perturbations propagate inward, a hard phase lag is produced. However, it is difficult to explain the transition frequency (e.g., 3.4 Hz for XTE J1550-564; 2.4 Hz for GRS 1915+105) where the lag converts from the hard type to the soft type. Qu et al. (2010) found that the frequency and phase lag are both energy dependent for the 0.5-10 Hz QPOs in GRS 1915+105. In XTE J1550-564, a similar type of complex variability is also observed (Cui et al. 2000). Reig et al. (2000) proposed that hard and soft lags are due to the mechanisms of Compton up-scattering and down-scattering. Basically, these mechanisms depend on gradient of temperature and optical depth of the plasma in the Comptonizing region. For low optical depth, only the up-scattering, i.e., positive lags are possible. For a large optical depth diffusion plus down-scattering open up the possibility of negative lags. In the Compton up-scattering model (Lee et al. 2001) soft lag is explained due to the Comptonization delays. Basically, these lags are due to the effects of the difference in the travel time of light and are comparable to the light crossing time of the objects. This lag does not switch sign, however. Poutanen & Fabian (1999) argue that the reflection of hard X-rays from the outer part of the accretion disk produces time delays that we may have already observed in Galactic black holes. In this case, the disk should be flared and the break in the time lag Fourier spectra would correspond to the size of the accretion disc.

Recently, using XMM data, Uttley et al. (2011) found in GX 339-4 that the softer disc photon lead the power-law photons at frequencies below  $\sim 1$  Hz. The lag behavior switches at frequencies above  $\sim 1$  Hz where softer disc photons start to lag the harder power-law photons. This behavior was interpreted as being due to the effect of the propagation (soft photon leads) to reverberation effects (soft photon lags). According to Arevalo & Uttley (2006), at small disc radii, an instability in accretion rate will cause a small variation only in disk emission inside that radius. This disc emission variability is dominated by X-ray heating effects which is due to the fluctuation in mass accretion at that radii.

In active Galactic nuclei, both hard and soft lags are explained with reverberation lag where reflection of Comptonized photons from the disc (Zoghbi et al., 2010; Wilkins & Fabian, 2013) are considered. Indeed, the switch in lag signature (a few tens milliseconds on short time scale variability) is consistent with the light-travel lags of reprocessed hard emission (power-law) from the soft (disc) emission at a few tens of gravitational radii. Since the Comptonization process could be the key reason for lags, it would be interesting to check if the size of this region, which is also responsible for QPOs, actually decides the amount of lags as the time lag is likely to be

proportional to the size of the Compton cloud.

In the context of the 1998 outburst of XTE J1550-564, a study of the phase-lag evolution during the initial rising phase was carried out by Cui et al. (1999, 2000). The magnitude of the lag was found to increase with the total X-ray flux. It was found that the QPO becomes stronger at higher energies (Cui, 1999; Chakrabarti & Manickam, 2000 for GRS 1915+105), which further supports the view that a QPO originates due to the oscillation of the Comptonizing region. although we consider only one each of high- and low-inclination sources, each with similar spectral and timing properties, the results may be general enough since there are many studies in the literature which indicate that these properties do have some inclination dependence. Munoz-Darias et al. (2013) and Heil, Uttley & Klein-Wolt (2015) showed that in higher inclination systems, there is systematically harder X-ray power-law emission. The properties of low-frequency QPOs are also inclination dependent. On the other hand, Heil et al. (2015) found that the amplitude of the broadband noise (subtracting the low-frequency QPOs) is no longer dependent on inclination, implying its correlation with the source structure of the emitting regions. Using Monte-Carlo simulations, Ghosh et al. (2011) also find that for the same disk flow properties that the spectrum changes with inclination angle.

There are yet other effects, such as the focusing of photons due to the gravitational bending of light from regions close to the black hole horizon, which could also be important and the delay introduced would be energy dependent as the energetic photons tend to be emitted from regions close to a black hole. In the present paper, for comparison, we study the time lag of one high inclination object namely, XTE J1550-564, and one low inclination object, namely, GX 339-4, for comparison. As we have discussed above, the result is likely to represent the whole class of objects with high and low inclinations, respectively. We explain the results of our observations by considering several effects on the time lag, namely, (i) repeated Compton scattering which introduces higher lags for higher-energy photons and for Compton clouds of larger size before they escape, (ii) reflection, and (iii) focusing due to gravitational bending. The structure of our paper is the following. In the Section 2, we discuss the properties of the two black holes under consideration. In §3, we present observational data and our analysis procedure. Specifically, we present the lag results for the XTE J1550-564 for which detailed studies of QPOs and spectral properties have already been presented in Papers I and II. We also include a similar study for GX 339-4. In §4, we present discussions of our results and provide an explanation of the behavior of the time lag. Finally, in §5 we provide our concluding remarks.

## 2. INTRODUCTION TO THE BLACK HOLE CANDIDATES UNDER CONSIDERATION

### 2.1. XTE J1550-564

The soft X-ray transient (SXT) XTE J1550-564 is one of the most interesting Galactic black hole candidate which has been studied over a broad range of wavelengths. The typical outburst behavior of XTEJ1550-564 during 1998 starts and ends in a low/hard state which is similar to the outburst profile of other black holes (e.g., GRO J1655-40, GX 339-4 etc.). This typical outburst be-

havior is supposed to be due to the sudden change in viscosity in the system (Hoshi 1979, Mandal & Chakrabarti, 2010). The time lag varies during the initial onset phase of 1998 outburst (Cui et al. 1999, 2000). The magnitude of lag increases with X-ray flux. The coherence is roughly constant and high (value is  $\sim 1$ ). Constant value is maintained up to the first harmonics of the Quasi Periodic Oscillations.

Properties of LFQPOs and spectral variability during 1998 outburst were reported in Papers I & II.

### 2.2. GX 339-4

The black hole candidate GX 339-4 is a low mass X-ray binary having a primary of mass  $\geq 6M_{\odot}$  (Hynes et al. 2003; Munoz-Darias et al. 2008) and it was first detected by the MIT X-ray detector on board OSO7 mission by Markert et al. (1973). Since its discovery, the source has exhibited four outbursts at 2 to 3 years intervals. The evolution of low-frequency quasi-periodic oscillations (QPOs) and spectral variability during 2010 outburst have been studied in detailed by Debnath et al. (2010, 2015) with Two Component Advective Flow model (TCAF) proposed by Chakrabarti & Titarchuk (1995; hereafter CT95) where they found that the QPO frequencies are monotonically increasing from 0.102 Hz to 5.69 Hz within a period of  $\sim 26$  days. They explained this evolution with the propagating oscillatory shock (POS) solution and find the variation of the initial and final shock locations and strengths. This behavior generally matches the values obtained from spectral fit with TCAF model (Debnath et al. 2015). With the TCAF model, a clear physical picture of what happens in an outburst emerges.

The only major difference between these two objects is the inclination angle. GX339-4 belongs to a class of low inclination ( $< 60$  deg) sources (Zdziarski et al. 1998) whereas XTE J1550-564 has a high inclination angle of  $74.7 \text{ deg} \pm 3.8 \text{ deg}$  (Orosz et al. 2011). However, both the sources exhibit a similar type of systematic evolutionary properties during the outbursts. Here we use this rich data set to study the evolution of lag variability during the outbursts.

### 3. OBSERVATIONAL ANALYSIS

We analyzed *RXTE* public archival observations of BHB GX 339-4 during 2007 outburst and observations covering the rising and declining phases of QPOs in 1998 outburst of XTE J1550-564 (for details, see, Paper I), limiting our analysis to observations when low frequency QPOs are observed. We produced background-corrected PCU2 rates in the Standard 2 channel bands A = 4-44 (3.3-20.20 keV), B = 4-10 (3.3-6.1 keV) and C = 11-20 (6.1-10.2 keV) and defined hardness ratio as C/B. We used Good Xenon, Event and Single Bit data modes which contain high time resolution data for timing analysis, which was performed using the GHATS software. For each observation we produced PDS every 16s in the channel band 0-35 (2-15 keV). We averaged them to obtain an average PDS for each observation and we subtracted the Poissonian noise contribution (Zhang et al. 1995). The PDSs were normalized and converted to fractional squared rms. The power spectra were then fitted with a combinations of Lorentzian (see, Nowak 2000) using XSPEC v 12.0.

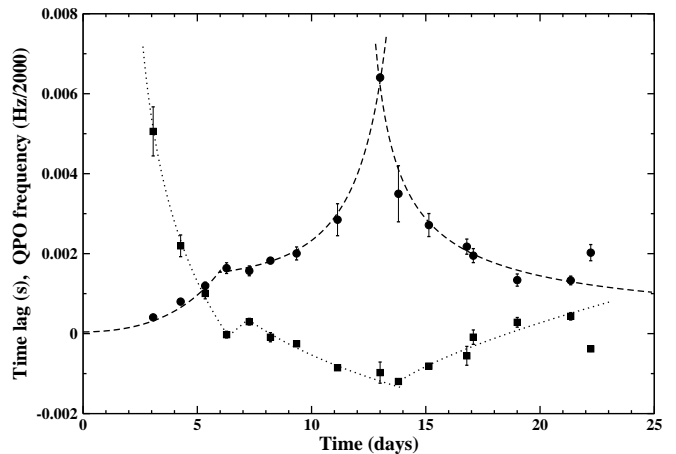


FIG. 1.— Evolution of time lag (filled squares) and QPO frequency (filled circles) are plotted with time (days) during rising (MJD 51065 to MJD 51076) and declining (MJD 51076 to MJD 51084) phases of XTE J1550-564 in the 1998 outburst. Time lag is calculated at QPO frequency ( $f_Q$ ) integrated over the width which is equal to FWHM ( $F_w$ ) of the QPO itself.

We also take the cross spectrum which is defined as,  $C(j) = X_1(j)^* X_2(j)$ , where  $X_1$  and  $X_2$  are the complex Fourier coefficients for the two energy bands at a frequency  $\nu_j$  and  $X_1(j)^*$  is the complex conjugate of  $X_1(j)$  (van der Klis et al. 1987). The phase lag between the signals of two different energy bands at Fourier frequency  $\nu_j$  is,  $\phi_j = \arg[C(j)]$  (i.e.,  $\phi_j$  is the position angle of  $C(j)$  in the complex plane.) and the corresponding time lag is  $\phi_j/2\pi\nu$ . An average cross vector  $C$  is determined by averaging the complex values for every stretches of time length. In our analysis, we produced a phase lag spectrum for each observation in our sample, dividing the data into two energy bands (2-5 keV & 5-13 keV) and extracting cross-spectra from 16s intervals, which are then averaged yielding one phase-lag spectrum per observation. Positive phase-lag indicates that the hard photons (5-13 keV) lag the soft photons (2-5 keV). Following Reig et al. (2000), we calculate QPO phase lag as the average of the phase lags over the interval  $\nu_c \pm FWHM$ , where  $\nu_c$  is the centroid frequency of the QPO and FWHM is its full width at half maximum as measured through a fit with a Lorentzian component.

#### 3.1. XTE J1550-564

Figure 1 shows the systematic variation of the time lag (filled squares), which is QPO frequency-dependent and the QPO frequency (filled circles) as a function of time (days) during the onset (MJD 51076-MJD 51084) and declining (MJD 51076-MJD 51084) phases of the 1998 outburst in XTE J1550-564. We consider the 0<sup>th</sup> day (i.e., MJD 51065) when the first QPO was detected. We studied the observations that cover the first three weeks of the outburst. In the onset phase, we fit time lag variation with a curve where the time lag  $\sim t^{-0.423 \pm 0.02}$  and the reduced  $\chi^2$  is close to 1.3 ( $\chi^2/10$ ). We find that time lag decreases with the increase of both the QPO frequency and time (day) during the onset phase. In the declining phase, we also find a systematic variation of the same time lag. The declining phase starts after observing the highest value of  $\nu_{QPO} = 13.1$  Hz on MJD 51076. The fitted curve represents time lag  $\sim t^{0.663 \pm 0.03}$  with a reduced  $\chi^2$  close to 1.6 ( $\chi^2/7$ ).

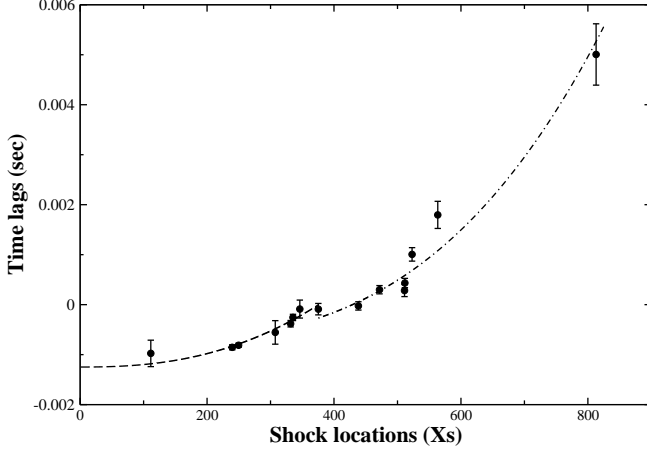


FIG. 2.— Variation of time lag with Shock location ( $X_s$ ) is plotted during the rising phase (MJD 51065 to MJD 51076) of XTE J1550-564 in the 1998 outburst. Time lag is calculated at the QPO frequency ( $f_Q$ ) integrated over the width equal to FWHM ( $F_w$ ) of the QPO itself.

In the TCAF solution, the QPO frequencies are derived from the inverse of the infall time in the post-shock region. According to the POS solution (Chakrabarti et al. 2008, 2009; Debnath et al. 2010, 2013), we can get an idea about the location of the shock wave ( $X_s$ ) from the observed QPO frequency ( $\nu_{QPO}$ ) as it is believed that QPOs are generated due to the oscillations of shock. The generated QPO frequency ( $\nu_{QPO}$ ) is proportional to the inverse of infall time ( $t_{infall}$ , i.e., light crossing time from the shock location to the black-hole), i.e.,  $\nu_{QPO} \sim (t_{infall})^{-1}$  and also  $t_{infall} \sim RX_s(X_s - 1)^{1/2} \sim X_s^{3/2}$   $R$  is the shock strength ( $= \rho_+/\rho_-$ , i.e., ratio of the post-shock to pre-shock densities.) Thus, QPO frequency according to this model,  $\nu_{QPO} \sim X_s^{-3/2}$ . The time dependent shock location is given by,  $X_s(t) = r_{s0} \pm vt/r_g$ , where  $v$  is the velocity of the shock wave. The positive sign in the second term is to be used for an outgoing shock and the negative sign is to be used for the in-falling shock.  $X_s$  is the measured units of the Schwarzschild radius  $r_g = 2GM/c^2$  where  $M$  is the BH mass and  $c$  is the velocity of light.

Accordingly, the shock location is larger for lower QPO frequency. The opposite is also true. In Fig. 2, variation of time lag (in seconds) with Shock location ( $X_s$ ) is plotted during the rising (MJD 51065 to MJD 51076) phases of XTE J1550-564 in the 1998 outburst. We clearly see that purely from observational point of view also, lag monotonically increases when QPO goes down and the derived shock location goes up. We thus have a fully consistent understanding that increase in QPO frequencies necessarily implies decrease in the size of the Comptonizing region. Even the ‘hiccup’ on day 6 in QPO frequency shows up in the lag profile also.

Because of the very nature of the physical processes by which high-energy photons are generated, the time lag must depend on the energy. First of all, repeated inverse Comptonization processes imply a higher time lag to generate higher energy photons. Similarly, focusing of emitted photons is also energy dependent since higher-energy photons are expected to come from regions closer to a black hole. This motivates up to compute energy dependence of the lag. Figure 3 shows energy dependent time lag for QPO centroid frequencies

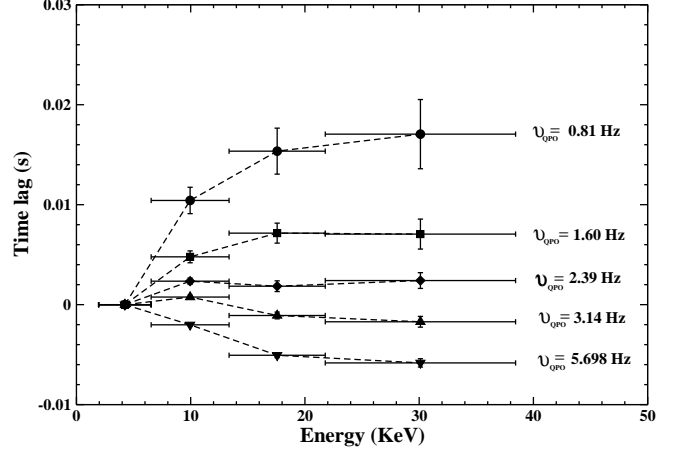


FIG. 3.— Energy dependent time lag (in seconds) for QPO centroid frequencies ( $f_Q = 5.698$  Hz,  $f_Q = 3.14$  Hz,  $f_Q = 2.39$  Hz,  $f_Q = 1.60$  Hz,  $f_Q = 0.81$  Hz) are plotted. We averaged time lag over the width equal to FWHM ( $F_w$ ) of the QPO itself. Here we calculated time lag w.r.t the reference energy band 1.94-6.54 keV (0-17, channels). The other energy bands are 6.54-13.36 keV (18-36, channels), 13.36-21.78 keV (37-59, channels) and 21.78-38.44 keV (60-103, channels).

$f_Q = 5.698$  Hz,  $f_Q = 3.14$  Hz,  $f_Q = 2.39$  Hz,  $f_Q = 1.60$  Hz,  $f_Q = 0.81$  Hz. We averaged time lag over the width equal to FWHM ( $F_w$ ) of the QPO itself. Here we calculated time lag w.r.t the reference energy band 1.94-6.54 keV (0-17, channels). The other energy bands are 6.54 – 13.36 keV (18-36, channels), 13.36 – 21.78 keV (37-59, channels) and 21.78 – 38.44 keV (60-103, channels). We find that lag could be positive or negative, depending on the QPO frequency and photon energy. This behavior suggests that the contribution to lag from different mechanisms vary with shock locations. Time lag monotonically increases with energy for QPO frequency 0.81 Hz, but monotonically decreases from a frequency of  $\sim 3.4$  Hz onward. The complex pattern of the phase lag associated with the QPO bear remarkable resemblance to that observed of GRS 1915+105 which is also high inclination source (Cui 1999, Reig et al. 2000). We shall discuss the physical cause in the final Section.

### 3.2. GX 339-4

We now turn to a source which belongs to a low-inclination binary system. If focusing by gravitational photon bending is important in deciding the lag, low inclination sources are not likely to be affected by this effect and the energy dependence of lag would look significantly different. This is precisely what we see in the source GX 339-4.

Figure 4 shows a systematic variation of the frequency dependent time lag as a function of day during the rising (MJD 51076 to MJD 51084) and the declining (MJD 54133 to MJD 54145) phases of GX 339-4 during the 2007 outburst. Time lag is calculated at the QPO frequency ( $f_Q$ ) in the same way as before.

Figure 5 shows variation of time lag with the shock location ( $X_s$ ) (computed from POS model) during the rising (MJD 54133 to MJD 54145) phase of GX 339-4 during the 2007 outburst. The Figure suggests that as QPO frequency increases, location of the shocks decreases, i.e., the size of the CENBOL is reduced systematically as the gradually weakening shock propagates towards the black hole.

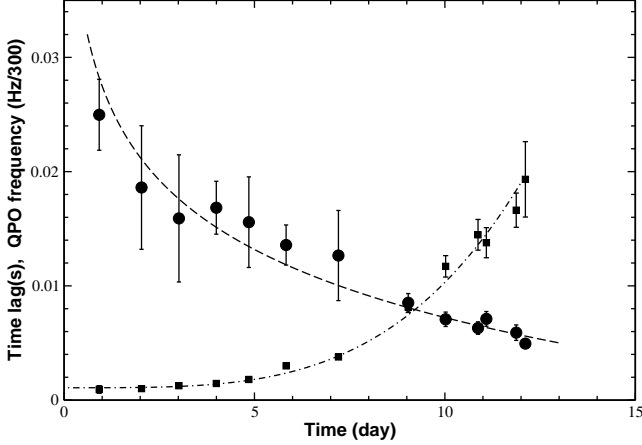


FIG. 4.— Evolution of time lag and QPO frequency are plotted as a function of time in days during the rising (MJD 54133 to MJD 54145) phases of GX 339-4 in the 2007 outburst. Time lag

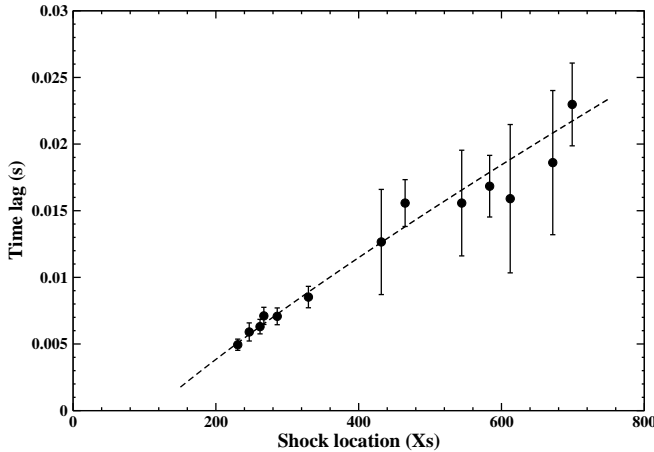


FIG. 5.— Variation of time lag with Shock location ( $X_s$ ) during the rising (MJD 54133 to MJD 54145) phase of GX 339-4 in the 2007 outburst. Time lag is calculated in the same way as in Fig. 2.

Figure 6 shows energy dependent time lag for QPO centroid frequencies  $f_Q = 6.87$  Hz,  $f_Q = 4.34$  Hz,  $f_Q = 4.14$  Hz,  $f_Q = 1.297$  Hz,  $f_Q = 0.436$  Hz. The time lag is calculated as before. Here we choose 2.0-5.4 keV (0-12, channels) as a reference energy band. The other energy bands are 5.4-6.9 keV (13-16, channels), 6.9-9.4 keV (17-22, channels), 9.4-13.1 keV (23-31, channels). We clearly find that energy dependent time lag depends on QPO frequency as well. We find hard lag to be monotonically increasing with energy of the photons for all the QPO frequencies. This behavior suggests that as the location of shock (i.e., QPO frequencies) changes, the contribution in total time lags that we observed from different mechanisms also changes. Furthermore, all the lags are positive, unlike the case of XTE J1550-564 which was of high inclination and contributions cancel to change sign at a particular shock location for a given object.

#### 4. DISCUSSION

So far, we have seen that the time lag is not only a function of the average energy of the emitted photons, it is also a function of the inclination angle of the binary system. What is clear in both high and low inclination

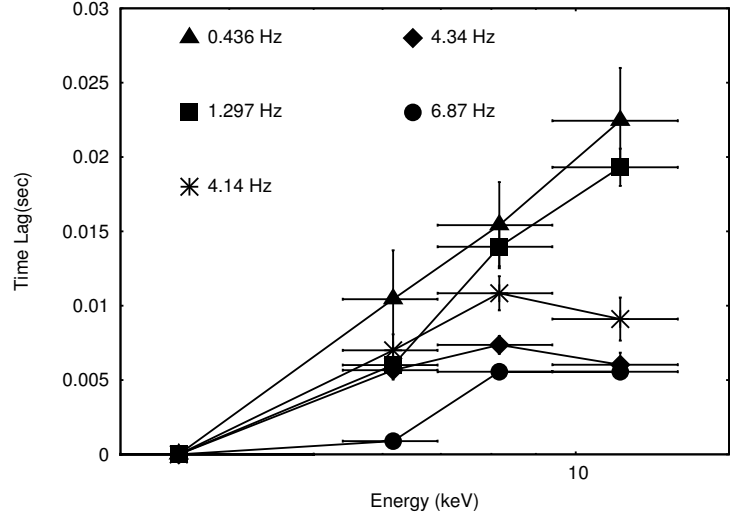


FIG. 6.— Energy dependence of time lag for different QPO centroid frequencies ( $f_Q = 6.87$  Hz,  $f_Q = 4.34$  Hz,  $f_Q = 4.14$  Hz,  $f_Q = 1.297$  Hz,  $f_Q = 0.436$  Hz). Here we choose 2.0-5.4 keV (0-12, channels) as a reference energy band. The other energy bands are 5.4-6.9 keV (13-16, channels), 6.9-9.4 keV (17-22, channels), 9.4-13.1 keV (23-31, channels). Clearly varies on QPO frequency. We find that the hard lag is directly related to the energy of photons for different QPO frequencies.

systems is that the lag increases when QPO frequency goes down, i.e., when the size of the Comptonizing region goes up. What is not obvious is the cause of change of sign at a specific QPO frequency, i.e., at a specific size. Below, we discuss the major processes which control the lag and give a possible reason of why the change of sign occurs only in high inclination systems.

##### 4.1. Evolution of Times lag and Quasi Periodic Oscillations

Typical evolutions of the QPOs in transient black-hole sources during outburst has already been established for a long time (Debnath et al. 2008, 2010, 2013; Dutta & Chakrabarti 2010; Chakrabarti et al. 2005, 2008, 2009). These evolutions suggest that certain specific physical mechanisms are in place which are responsible for the generation of QPOs for days after days (Chakrabarti et al. 2005, 2008, 2009; Debnath et al. 2008, 2010, 2013). These authors found that the Comptonization region gradually shrinks in the rising phase of an outburst when QPO frequencies go up and the reverse is true in the declining phase. We would also expect that, in general, there would be a monotonically decreasing lag with increasing QPO frequency and a monotonically increasing lag with shock location. This is precisely what happens in both the objects: the net time lag due to Comptonization is the sum over light crossing times of the mean free paths  $l_{Comp}$  between two successive Compton scatterings, i.e.,  $t_{lag}^c = \sum l_{Comp}/c \propto X_s/c$ . However, when one considers the energy dependence, the picture is more complex. Since energy is expected to rise, after each successive scattering, higher energies are expected to have higher lags. As pointed out by earlier workers (Cui, 1999; Cui et al. 2000; Reig et al. 2000) have pointed out, we also find that the energy dependence of the time lag is not straightforward to understand. In XTE J1550-564 (Cui et al. 2000) the lag first increases with frequency, peaks at some characteristic frequency,

and then decreases and moves toward to negative (soft) lag at frequency  $\sim 3.4$  Hz. This pattern of the phase lag associated with the QPO bears a remarkable resemblance to that observed in GRS 1915+105 (Cui 1999; Reig et al. 2000), albeit with ‘zero-lag’ occurring at a different QPO frequencies. This is due to the very nature of the emission process in both the Keplerian and sub-Keplerian components.

The physical processes contributing to lags may be understood from Fig. 7 where we show how the radiations from an accretion disc and Comptonizing cloud (CENBOL) may reach observers located at an angle  $\theta \lesssim 60$  deg and  $\theta \gtrsim 60$  deg through various paths. As already mentioned, the time of travel is proportional to the number of scattering at the CENBOL and one expects harder X-rays (HXR) to come at later times. However, radiations emitted from inner CENBOL (CENBOL-B) are also focussed due to gravitational bending of lights and may be further delayed. Hard photons reflected from the Keplerian disc as softer radiation (RSXR) also takes a longer route, especially for high inclination sources. Thus, while each soft photon may have a range of time lag (high and low) depending on whether it is focussed and/or reflected before reaching the observer, hard X-rays are always expected to be delayed. This causes non-monotonicity of the lag with energy when the inclination angle is high. Qualitative behavior could be understood from Fig. 8 where we schematically plot the time lag ( $t_{lag}$ ) as a function of the size of the Comptonizing region ( $R_c$ ), believed to be located at the inner region (Chakrabarti & Titarchuk, 1995). We plot this for  $\theta \lesssim 60$  deg on the left and for  $\theta \gtrsim 60$  deg on the right. The boundary of this region (CENBOL) is the shock location  $X_s$ . For convenience, we assume CENBOL is divided into two gross parts: CENBOL-A emits relatively softer photons than CENBOL-B. Lag due to Comptonization (super-script ‘c’) of hard X-rays (HXR) would be proportional to the number of scattering which took place. Roughly, therefore, the energy would monotonically increase linearly with the size and its lag will also increase ( $dt_{HXR}^c$  in Fig. 8). Soft X-rays from the Keplerian disc will not be strongly affected by the size of the CENBOL. Hence, in Fig. 8,  $dt_{SXR}^K \sim 0$ , always. When  $\theta \lesssim 60$  deg, the focusing and reflection effects are also negligible. So, we expect the lag  $dt_{HXR}^c - dt_{SXR}^K$  to be always positive in this case (left panel of Fig. 8). However, when the inclination is high ( $\theta \gtrsim 60$  deg), apart from the above two lags, we have monotonically decreasing effects of soft ( $dt_{SXR}^F$ , big circled curve; from CENBOL-A) and hard X-ray ( $dt_{HXR}^F$  squared-curve; from CENBOL-B) lags due to focusing by gravitational bending effects. These are shown in the right panel of This is because bending is important only when the emission is closer to the black hole. Focusing is expected to cause a delay of the order of  $1 - 2r_g/c$  for hard X-rays (from CENBOL-B) and  $5 - 10r_g/c$  for soft X-rays (CENBOL-A) since they must be proportional to the size of the emitting region of corresponding radiations. Thus, the lag due to focusing of soft X-rays is on an average higher. The reflection component is a reprocessed CENBOL emission from the Keplerian disc and is a relatively softer radiation. The delay goes up linearly with the size of CENBOL ( $dt_{SXR}^R$ , small circled curve in right panel of Fig. 8) and the inclination

angle. The combination of these four effects could result in interesting patterns. In the right panel of Fig. 8, we draw the total delay of hard X-rays (solid curve  $dt_{HXR}^t$  which is the sum of  $dt_{HXR}^c$  due to Comptonization and  $dt_{HXR}^F$  due to focusing) and the total delay of soft X-rays (solid curve  $dt_{SXR}^t$  is the sum of  $dt_{SXR}^K$  from the Keplerian disc,  $dt_{SXR}^c$  due to Comptonization,  $dt_{SXR}^F$  due to focusing and  $dt_{SXR}^R$  due to reflection), here we have assumed that no flare like situation (unless flashes like solar flares; rare in persistent sources) occurs where hard X-rays could perhaps be expected earlier than the down scattered soft X-rays. So we did not bring this issue at all. These two solid curves intercept at  $R_c = R_{tr}$  below which the lag ( $dt_{HXR}^c - dt_{SXR}^t$ ) is negative. This means that according to TCAF, there is a cross-over QPO frequency (inverse of the infall time of matter from  $R_{tr}$  to the horizon) above which the hard lag would be negative. This cross-over frequency clearly depends on the mass of the black hole which determines the length scales and time scales of the disc components and the CENBOL.

Heil et al. (2015) analyzed a large number of black hole candidates and found that higher inclination sources with the same power spectral shape (in PDS) exhibit systematically harder X-ray power-law emission. Though they found that the broad band noise in the power density spectrum is independent of inclination angle, Type-C QPOs, located at different regions of the spectrum are found to be inclination dependent. They conclude that this property strongly depends on the inclination angle. In soft states, there are no low frequency QPOs and there is no distinction with inclination angle. Munoz-Darias et al. (2013) found that marginally soft states will be marginally harder in high inclination systems. In other words, hardening of spectrum is due to higher abundance of harder radiation in relation to soft radiation. This is precisely what happens in Fig. 7. Ghosh et al. (2011) found that the same outgoing photons from Monte-Carlo simulations when binned with respect to inclination angles, distinctly showed harder spectra at higher inclinations.

Our present work establishes this property more firmly using timing analysis. Here we considered two sources which show very similar systematic evolution in QPOs and spectral states. In XTE J1550-564, QPO frequency rises from 0.01 Hz to 14.0 Hz and starts to fall in the declining state. During this time, the shock location also vary from  $\sim 800$  to  $\sim 100$ . Also, from spectral studies with TCAF we find a similar changes in the Compton cloud size (CENBOL). In GX 339-4, QPO frequencies vary from 0.10 Hz to 5.69 Hz and then monotonically decreases, whereas the shock location changes from  $\sim 600$  to  $\sim 200$  (Debnath et al. 2010; Nandi et al. 2012). The complex outburst profiles of both the sources exhibit similar spectral evolution: hard  $\rightarrow$  hard-intermediate  $\rightarrow$  soft-intermediate  $\rightarrow$  soft  $\rightarrow$  in rising state and in reverse order in the declining state (Debnath et al. 2008). Moreover, they have comparable masses while differing only in inclination which affected the QPOs and the phase lags in the same way. Thus, our conclusion is expected to be valid for not just the two sources under consideration, but also for the two classes of sources, one with high and the other with low inclination.

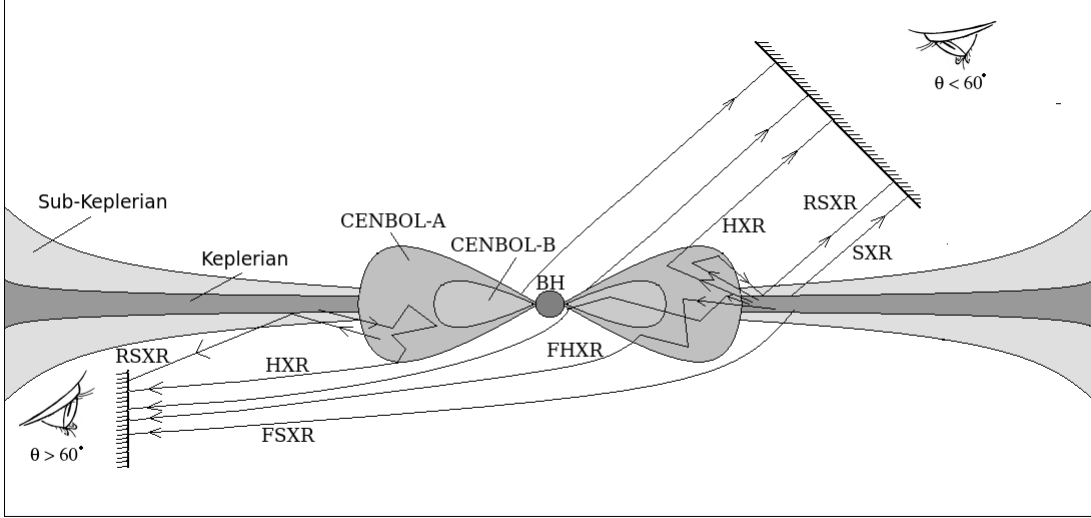


FIG. 7.— Cartoon diagram of two component advective flows where soft photons (SXR) from Keplerian discs are inverse Comptonized by the post-shock region, namely, Centrifugal pressure supported BOUNDARY Layer (CENBOL) and hard X-rays (HXR) are produced. Radiations can directly reach the observer, or reach through focusing effects (FSXR, FHXR). Harder radiations from the inner regions of CENBOL (CENBOL-B), would be more focussed than the Comptonized photons which had undergone lesser number of scattering from outer CENBOL (CENBOL-A). Reflected component (RSXR) from a Keplerian disc would primarily affect softer X-rays and may delay soft X-ray travel time. Observers with  $\theta \lesssim 60$  deg will see lesser focusing effects.

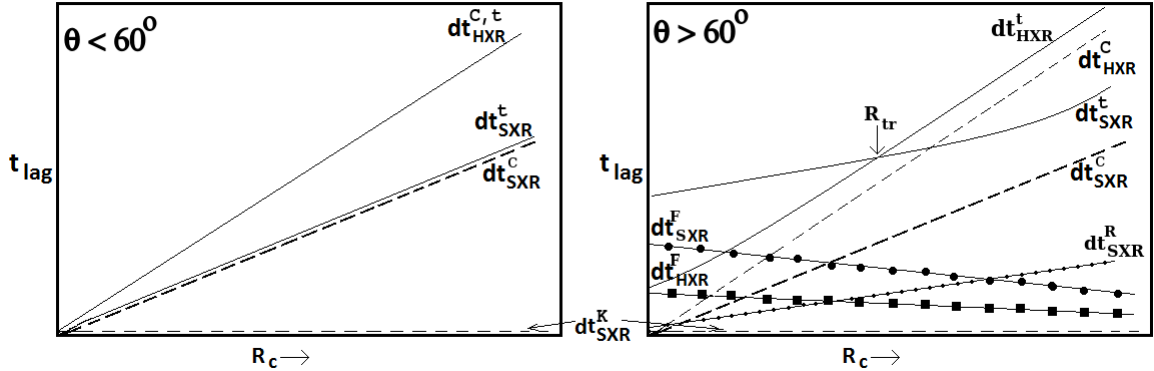


FIG. 8.— Schematic diagram explaining inclination angle and energy dependence of time lag. We consider two cases:  $\theta \lesssim 60$  deg (left) and  $\theta \gtrsim 60$  deg (right). In the former case, only Comptonization is important. In latter case, Comptonization, reflection and focussing are important. As a result, the lag may change sign at a given frequency of the power density spectrum. See text for details.

## 5. CONCLUSIONS

In the present paper, we extended the earlier studies in Paper I and Paper II to understand the behavior of time/phase lag property of the black hole candidate XTE J1550-564. Property of this high inclination object was contrasted to those of a low inclination black hole candidate, namely, GX 339-4. We concentrated on the lag at the QPO frequencies as the oscillation is more coherent and lag measurement is less erroneous. In this paper, we have used the TCAF paradigm for the explanation of time lag properties primarily because only in this paradigm, there is a distinct prediction among time lag, size of the Compton cloud, QPO frequency and spectral states. To our knowledge no other model in the literature such as the disk corona model (Haardt & Maraschi, 1993; Zdziarski et al., 2003) and lamp-post models (Martocchia & Matt 1996; Miniutti & Fabian 2004) actually bring out such relations naturally. We found that in both the cases, the lag at QPO frequency generally rises as the frequency goes down. In fact, exactly opposite result is

found also in the declining phase. In a TCAF solution, this implies that the lag would increase as the size of the Comptonizing region increases. This is precisely what we see also. However, the dependence of lag on photon energy is more intriguing. We find that GX 330-4 exhibits only positive lag for all QPO frequencies, while in XTE J1550-564, the lag switches sign and it becomes negative above certain frequency. We discussed major effects which could be controlling the property of the lag. Specifically, we showed that if we add up the qualitative variations of the lag components, then the high inclination objects could have negative time lags, i.e., soft photons appearing after hard photons due to reflection and focussing effects. We see this effect in XTE J1550-564 at frequencies higher than  $\sim 3.4$  Hz. This frequency gives rise to a characteristic length-scale ( $R_{tr}$ ) where the lag changes its sign. Most certainly, this frequency is not universal as the cancellation of lags would depend on inclination angles and the mass of the black holes which determine the length scales. Indeed, in another object, namely, GRS1915+105, having a mass at least twice as

much, the transition frequency happens to be lower (2.2 Hz). Detailed work is in progress and would be presented elsewhere.

## 6. ACKNOWLEDGEMENTS

This research has made use of RXTE data obtained through HEASARC Online Service, provided by the

NASA/GSFC, in support of NASA High Energy Astrophysics Programs. We thank T. Belloni for providing the timing analysis software GHATS at X-ray Astronomy School (IUCAA, Pune). Also, B. G. Dutta acknowledges the support of UGC (Minor Research Project) to carry forward his research works.

## REFERENCES

- Arevalo P. & Uttley P., 2006, MNRAS, 367, 801  
 Botcher, M. & Liang, E. P., 1999, ApJL, 511, L37  
 Chakrabarti, S. K., Nandi, A., & Debnath, D., et al., 2005, IJP, 79(8), 841 (arXiv:astro-ph/0508024)  
 Chakrabarti, S.K., Debnath, D., & Nandi, A., et al., 2008, A&A, 489, L41  
 Chakrabarti, S.K., Dutta, B.G. & Pal, P.S., 2009, MNRAS, 394, 1463C  
 Chakrabarti, S.K. & Titarchuk, L.G., 1995, ApJ, 455, 623  
 Chakrabarti, S.K., Mondal, S., Debnath, D., 2015, MNRAS, 452, 3451C  
 Chakrabarti, S.K. and Manickam, S. 2000, ApJ, 531, 41  
 Cui, W., Chen, W., & Zhang, S. N., 1999, ApJ, 484, 383  
 Cui, W., 1999, ApJ, 524, L59  
 Cui, W., Zhang, S. N., & Chen, W., 2000, ApJ, 531, L45  
 Debnath, D., Chakrabarti, S. K. & Nandi, A., 2010, A&A, 520A, 98D  
 Debnath, D., Chakrabarti, S. K., & Nandi, A., et al., 2008, BASI, 36, 151  
 Debnath, D., Chakrabarti, S.K., & Nandi, A., 2013, AdSpR, 52, 2143  
 Debnath, D., Mondal, S., & Chakrabarti, S.K., 2015, MNRAS, 447, 1984  
 Dutta, B.G. & Chakrabarti, S. K., 2010, MNRAS, 404, 2136D  
 Ghosh, H., Garain, S. K., Giri, K., & Chakrabarti, S. K., 2011, MNRAS, 416, 959G  
 Haardt, F., & Maraschi, L., 1993, ApJ, 413, 507  
 Heil, L. M., Uttley, P. & Klein-Wolt, M., 2015, MNRAS, 448, 3348  
 Hoshi, R., 1979, Progress of Theoretical Physics, 61, 1307  
 Hynes R. I., Steeghs D., Casares J., Charles P. A., O'Brien K., 2003, ApJ, 583, L95  
 Lee, H. C., Misra, R. & Taam, R. E., 2001, ApJ, 549L, 229L  
 Lightman, A. P. & Eardley, D. M., 1974, ApJ, 187, L1  
 Lin, D., Smith, I. A., Liang, E. P. & Botcher, M., 2000, ApJ, 543L, 141  
 Lyubarskii, Yu. E., 1997, MNRAS, 292, 679  
 Mandal, S. & Chakrabarti, S.K., 2010, ApJ, 710, L147  
 Markert T. H., Canizares C. R., Clark G. W., Lewin W. H. G., Schnopper H. W. et al., 1973, ApJ, 184, L6  
 Martocchia, A. & Matt, G. 1996, MNRAS, 282, L53  
 McClintock, J. E., & Remillard, R. A., 2006, in Compact Stellar X-ray Sources, ed. W. Lewin & M. van der Klis, 39, 157  
 Miniutti, G. & Fabian, A. C. 2004, MNRAS, 349, 1435  
 Miyamoto S., Kitamoto S., Mitsuda K., Dotani T., 1988, Nat, 336, 450  
 Muoz-Darias, T., Casares, J. & Martinez-Pais, I. G., 2008, MNRAS, 385, 2205  
 Munoz-Darias T., Motta S., Belloni T. M., 2011, MNRAS, 410, 679  
 Muoz-Darias, T., Coriat, M. & Plant, D. S., 2013, MNRAS, 432, 1330  
 Nandi, A., Debnath, D., & Mandal, S., et al., 2012, A&A, 542, 56  
 Nowak, M. A., Wilms, J., Dove, J. B. 1999, ApJ, 517, 355  
 Nowak, M. A., 2000, MNRAS, 318, 361  
 Orosz, J. A., Steiner, J. F., McClintock, J. E., Torres, M. A. P., & Remillard, R. A., et al., 2011, ApJ, 730, 75O  
 Payne, D. G., 1980, ApJ, 237, 951  
 Poutanen, J., 2001, in X-RAY ASTRONOMY: Stellar Endpoints, AGN, and the Diffuse X-ray Background. Edited by Nicholas E. White, Giuseppe Malaguti, and Giorgio G.C. Palumbo. AIPC, 599, 310  
 Poutanen, J. & Fabian AC, 1999, MNRAS, 306, L31  
 Qu, J. L., Lu, F. J., & Lu, Y. et al., 2010, ApJ, 710, 836  
 Reig, P., Belloni, T., van der Klis, M., Mendez, M. & Kylafis, N.D., 2000, ApJ, 541, 883  
 Remillard R., McClintock J., 2006, ARA&A, 44, 49  
 Shakura, N. I. & Sunyaev, R. A., 1976, MNRAS, 175, 613  
 Uttley, P., Wilkinson, T. & Cassatella, P. et al. 2011, MNRAS, 414L, 60  
 van der Klis, M., Hasinger, G., Stella, L., Langmeier, A., van Paradijs, J., & Lewin, W. H. G. 1987, ApJ, 319, L13  
 van der Klis M., 2004, Advances Space Res., 34, 2646  
 Wilkins, D. R. & Fabian, A. C., 2013, MNRAS, 430, 247  
 Zdziarski, A. A., Poutanen, J., Mikolajewska, J., Gierlinski, M., & Ebisawa, K., et al., 1998, MNRAS, 301, 435  
 Zdziarski, A. A., Lubinski, P., & Gilfanov, M., et al., 2003, MNRAS, 342, 355  
 Zhang, W., Jahoda, K., Swank, J. H., Morgan, E. H. & Giles, A. B., 1995, ApJ, 449, 930  
 Zoghbi, A., Fabian, A. C., Uttley, P., Miniutti, G., & Gallo, L. C et al., 2010, MNRAS, 401, 2419